

**Table of contents**

<b>NSPIRES Cover Sheets</b>	<i>i</i>
<b>Table of contents</b>	<i>xxiii</i>
<b>1. Scientific/Technical/Management Section</b>	<i>1</i>
<b>1.1 Scientific rational and objectives</b>	<i>1</i>
1.1.1 Introduction and observations	<i>1</i>
1.1.2 Preliminary work on crater population	<i>3</i>
1.1.3 Additional Constraints from HiRISE stereo DEMs	<i>6</i>
1.1.4 Proposal Objectives and Tasks	<i>6</i>
<b>1.2 Technical approach and methodology</b>	<i>12</i>
1.2.1 Update population statistics	<i>12</i>
1.2.2 Crater thermal model	<i>12</i>
1.2.3 Evolution of a single crater	<i>13</i>
1.2.4 Accumulation and modification of crater populations over 20Kyr	<i>14</i>
1.2.5 NRC suncup formation modeling	<i>14</i>
1.2.6 Application of results to the NPLD and lower latitude craters	<i>14</i>
<b>1.3 Expected significance and relevance to NASA goals</b>	<i>14</i>
<b>1.4 Work plan and team roles</b>	<i>15</i>
<b>2. References</b>	<i>16</i>
<b>3. Facilities and equipment</b>	<i>19</i>
<b>4. Curricula Vitae</b>	<i>20</i>
<b>5. Current and pending support</b>	<i>23</i>
<b>6. Budget</b>	<i>26</i>
6.1 Budget Justification	<i>26</i>
6.2 Budget Amounts	<i>28</i>

## 1. Scientific/Technical/Management Section

### 1.1 Scientific rational and objectives

#### 1.1.1 Introduction

The North Polar Layered Deposits (NPLD) are a multi-kilometer thick sequence of dusty-ice layers thought to record previous climatic conditions much like Earth's ice sheets record terrestrial climate fluctuations in their stratigraphy. Deciphering this polar record has been, and remains today, a major goal of Mars research. Observations by the Mars Reconnaissance Orbiter (MRO) and other recent missions have enabled seminal advances in understanding the polar deposits as relevant to Martian climatic history. We now know that their dust-content is less than a few percent and that internal layers are contiguous across the entire deposit (Phillips et al., 2008). Internal layering has been imaged at high-resolution where it is exposed in the many troughs and scarps within the NPLD. Comparisons of these exposures with solutions of past orbital change (Laskar et al. 2004) have suggested a link between a ~30m wavelength periodicity in the stratigraphy to variation of Mars' argument of perihelion (a 51Kyr cycle) (Laskar et al., 2002; Milkovich and head, 2005; Milkovich et al., 2008). Although this stratigraphic periodicity remains controversial e.g. Perron and Huybers (2009) and the exposures themselves may not be characteristic of the internal layering (Herkenhoff et al., 2007).

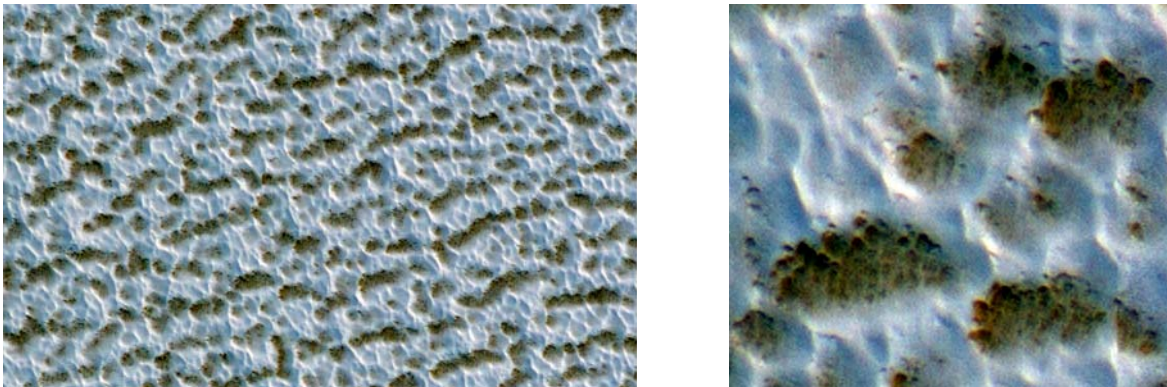


**Figure 1.** HiRISE view of a typical NRC surface showing fine-grained water ice overlying a darker substrate. Individual darker/lighter patches are ~10m across. Right panel shows a closer view of the NRC texture. Within the darker area the small pits are ~1m across.

In concert with these advances in understanding the stratigraphic record, we now have several years of monitoring of the current martian climate by spacecraft. Quantities such as atmospheric temperatures (McCleese et al. 2008), atmospheric humidity as a function of location and time (Smith, 2008), dust storm frequency and cloud activity are becoming better constrained.

*Therein lies the gap in our current knowledge.* We know something of the stratigraphy laid down by previous climates; however, the climatic conditions themselves and their affect on polar deposition can be investigated only with models (e.g. Levrard et al. 2007). We also know something of the current climate, yet we do not know today what the accumulation rate on the NPLD is (or whether it is accumulating at all). The actual connection between polar stratigraphy and climate remains elusive.

NPLD deposition today is thought to occur through the northern residual ice cap (NRC). The NRC is dominated by decameter scale light dark patches (Thomas et al. 2001) as can be seen in figure 1. Visual and hyperspectral data show the NRC is composed of clean large-grain water ice (Kieffer 1990; Langevin et al. 2005). Ice-grain size increases with time so the observation of large ice-grain sizes implies that old ice is being exposed during the summer, which would mean

that the NRC is currently undergoing a net loss of material. However over the past 10 Kyr, the theoretical expectation is that mid-latitude ground ice has been retreating and reaccumulating on the polar cap as the argument of perihelion has changed (and with it polar climate, see figure 2) (Chamberlian and Boynton, 2007; Schorghofer et al. 2007). Likewise, general circulation models of the transport of water vapor between north and south poles over the past 100Kyr (Montmessin et al. 2007) predict that water ice could be transported from the NPLD to the south pole between 10 and 34Kyr ago and that water ice should reaccumulate at the north pole over the past 10Kyr. Independent calibration of the NRC accumulation rate is unfortunately lacking. A Viking-image search uncovered no impact craters (Herkenhoff and Plaut, 2000) larger than 300m on the NRC surface indicating a surface age  $< 100$ Kyr while Tanaka (2005) argued for a surface age of 8.7Kyr based on knowledge of only two craters. To complicate matters further, the extent of the NRC also varies interannually (Malin and Edgett 2001; Hale et al. 2005). These variations are limited to a few percent of its area and seem reversible on timescales of years (Byrne et al. 2008a).

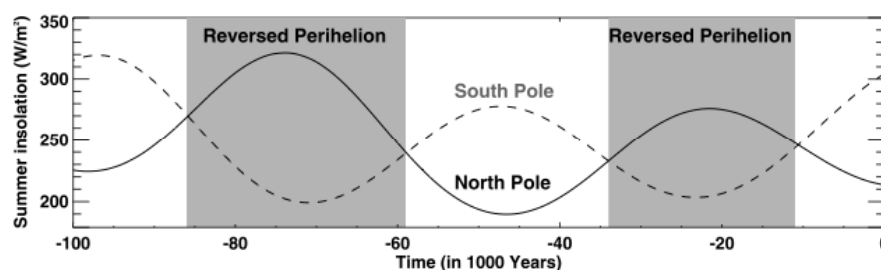


**Figure 2.** Orbital solutions of Laskar (2004) for the past 100 Kyr allows calculation of peak insolation at each pole. Figure from Montmessin et al (2007).

In short, we may have had a recent period of NPLD accumulation (lasting  $\sim 10$ Kyr) coincident with a recent downturn in north polar insolation (figure 2) that has just ended (allowing older large-gained ice to be exposed by ablation). We have very few constraints from the previous work on impact craters and no knowledge of how much accumulation may have occurred in this era. Accumulation may have stopped decades, centuries or a millennium ago and there are no in situ measurements of basic meteorological quantities on the polar cap itself (Phoenix landed about 1300km from the pole). In addition it is not clear why accumulation may have recently stopped while north polar insolation continues to decrease.

The current mass balance of the NRC was identified as a critical piece of information to link polar stratigraphy to climate by several recent reviews (Titus et al. 2008; Fishbaugh et al. 2008; Byrne 2009) and the 2008 MEPAG report. Indeed, a recommended investigation of this report reads: “*Understand how volatiles and dust exchange between surface and atmospheric reservoirs, including the mass and energy balance. Determine how this exchange has affected the present distribution of surface and subsurface ice as well as the Polar Layered Deposits*”.

**This proposal aims to quantify the accumulation rate of the NPLD and how it has changed over the past 10-20Kyr independent of climate models and thus provide a link between a climate we understand (today’s) and climatic conditions we do not (but which are recorded in the NPLD stratigraphy).**

To do this we make use of new sources of information. The Context Camera (CTX) on board MRO has acquired complete coverage of the NPLD at  $\sim 6$ m/pixel. We have searched these publicly-available data and discovered and measured over 100 craters (Banks et al., 2010). These results will be summarized in the following section and allow us to deduce the crater removal rate. Recent advances in refining the martian cratering rate (Hartman 2005), including

the effects of atmospheric screening (Popova et al. 2003), have improved these estimates. They agree well with small-crater counts (Kreslavsky 2009) conducted elsewhere on Mars.

We will model the degradation and infilling of these craters through ablation and condensation of water ice using the timescale constraints supplied by the crater population statistics we have measured. Once our model accurately describes the removal of craters we will apply it to the surrounding flat terrain and deduce the resurfacing rate that implies. As will be described below, this crater population is recording accumulation over the past 10-20Kyr. In contrast to purely theoretical studies, we will not need to make assumptions about how climate varies in response to changing orbital elements. Instead, we can solve for this by matching a modeled population of craters to the population-statistics we have observed.

Additional resurfacing processes apply to the NRC that do not strongly affect accumulation within craters. The current surface of the NRC is dominated by an approximately decameter scale texture of mounds of bright water frost on top of a darker (larger-grained & older) substrate (figure 1). At smaller scales, the surface of the NRC also shows abundant suncups ~1m in diameter. Suncup scale in terrestrial snow is related to the penetration depth of incident solar radiation. We will adapt and improve an existing model (Tiedje et al. 2006) for suncup formation and investigate the implications for the packing density, age and dust-content of the uppermost surface. Thus we can relate the properties of the upper decimeters of the NRC to today's insolation, humidity and dust-storm activity.

**Data Availability:** The work described in section 1.1.2 and proposed throughout the following sections is based on analysis of data acquired by MRO last northern-hemisphere summer (during 2008) before the onset of the polar hood. The most recent of these data have been publicly available via the PDS since 3/2009 (in the case of HiRISE) and 6/2009 (in the case of CTX), both much longer than the required 30 days before proposal submission.

We will also utilize high-resolution DEMs, produced by the HiRISE team from stereo imagery, of some of these craters to further constrain our models. The most recent of these DEMs was archived by the HiRISE team in the PDS on August 2<sup>nd</sup> 2010.

### 1.1.2 Preliminary work on identifying craters

As part of a previous MDAP grant (now completed) we examined all CTX, MOC and THEMIS images of the NPLD to search for impact craters and analyzed their population statistics. The findings of this study in large part motivated this proposal and so the most relevant points will be briefly reviewed here. These results are published as Banks et al. (2010).

The CTX camera has now achieved complete coverage of the NPLD at 6m/pixel and all these data are available from the PDS. In examining these data we mapped the positions of over 100 impact craters up to 450m in diameter. It is immediately obvious from the low number of craters and their small size that this is a very young/geologically-active surface. The NPLD is comprised of large flat areas mostly covered with residual ice interspaced with troughs and scarps that expose its layered interior. While the flat areas are likely sites of recent deposition, the sloping trough walls are not (or else the layered-exposures would be covered). In the past, researchers have used the bright residual ice as a proxy for areas of recent accumulation (Tanaka 2005); however, we now know that its extent varies from year to year. We also know it is quite thin (likely decimeters) and so craters within patches of residual ice on the surrounding Vastitas Borealis plains do not superpose the residual ice but instead belong to the plains unit. To avoid these issues we defined a region of recent accumulation using the MOLA DEM data. We included terrain on the topographic dome of Planum Boreum that passed a certain smoothness

criterion (which excluded dunefields). To avoid including layered trough walls we excluded terrain with a poleward slope  $> 7^\circ$  or equatorward slope  $> 1^\circ$ . The resulting region (Figure 3) has an area of 0.7 million  $\text{km}^2$  and is a close match to the NRC but includes flat and poleward sloping areas on Planum Boreum currently free of residual ice and excludes areas of the surrounding Vastitas Borealis unit that do currently have thin covers of residual ice.

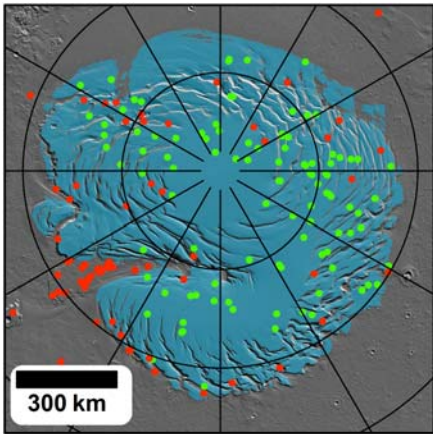
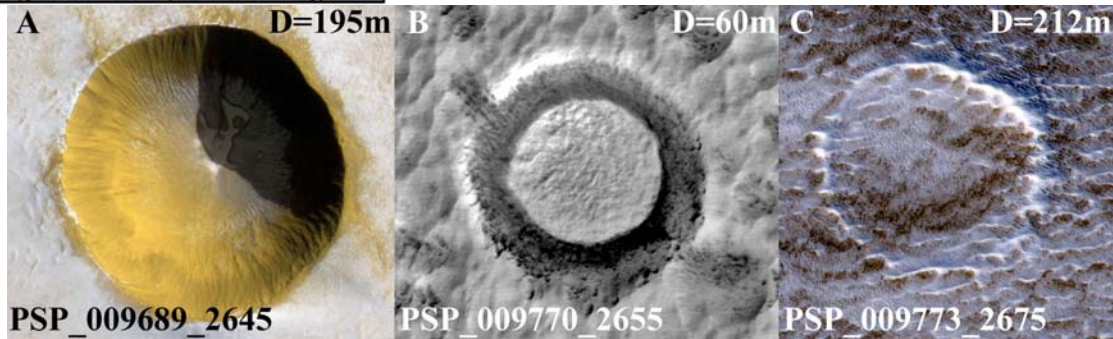


**Figure 3.** Left panel shows study area of Banks et al. (2010) in blue (parallels and meridians are spaced 5 and 30 degrees apart respectively). Green dots shows crater locations within the study area while red dots are craters that occur outside this area or on trough walls etc... Lower panels are HiRISE sub-images showing three example craters on the NRC with increasing levels of infilling. Crater diameter indicated in upper-right of each panel.



Within this region, 103 craters were identified with diameters ranging from  $\sim 10$ -352m. These craters form a continuous series from those that are highly degraded to those that are relatively fresh (see Figure 3). Even the freshest of these craters (Figure 3A) shows a sublimation lag already in place on the steep crater walls which is slumping downslope and covering up the small patch of bright ice still visible on the crater floor. These craters are preferential sites of ice accumulation in that the ice within them is typically brighter than the surrounding NRC (indicating that it is fine-grained and young). Some craters appear to have accumulating ice within them even though the terrain surrounding the crater defrosts entirely in the late summer (figure 4). The pervasive decameter scale texture of the NRC overprints older crater rims leading to their destruction (Figure 3C) in addition to the meter-scale suncups that form on the crater walls and surrounding terrain. The range of morphologies and continuum of states of infill indicate that many craters have likely been removed completely by these processes, a conclusion which the population statistics support.

It can be seen from figure 5 that this population of craters does not follow a production function (the inclined dashed lines represent the 5, 10, and 20 Kyr isochrons). Our crater population is deficient in small craters relative to that expected i.e. the slope of the size-frequency curve is shallower than the production curve. The slope fit to our size-frequency distribution was -1.89 for the cumulative and -1.85 for the differential plot whereas a fit to the data tabulated in Hartmann [2005] in this diameter range shows the isochron slopes to be -3.04 and -2.99 respectively (this slight mismatch is the result of incorporating atmospheric screening

of projectiles). Such behavior can be explained in terms of an equilibrium population where craters are being removed on a timescale comparable to that over which they accumulate. In the case of the differential representation, the product of the crater production function (which is diameter dependent) and the crater lifetime (also diameter dependent) creates the size-frequency distribution of craters we see today. Taking power-law fits to the isochrons and the observed size-frequency distribution, we find that crater lifetime is  $30.75 \cdot D^{1.14}$  years ( $D$  is crater diameter). Thus for example, a 100m crater on the NPLD is removed in 5.9 Kyr.

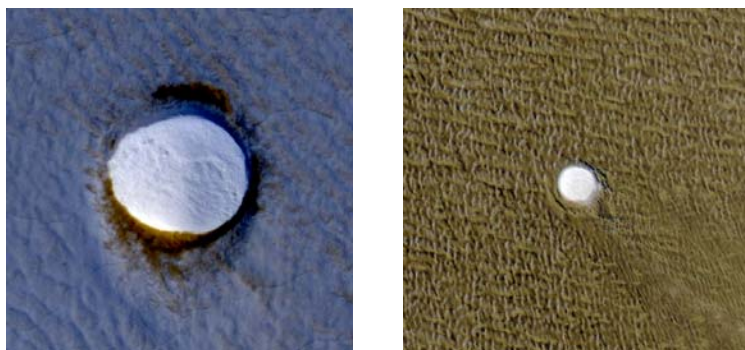


**Figure 4.** HiRISE images PSP\_009404\_2635 (left) and PSP\_009223\_2640 (right) showing craters with interior ice deposits. The ice within craters is brighter than surrounding ice (left) and can accumulate even when surrounding ice is unstable (right).

An equilibrium surface cannot be ‘dated’ with a single age (as the length of time represented by the craters depends on what size of crater you consider). A surface may remain in this equilibrium state for an arbitrarily long period of time; however, we can constrain a minimum amount of time the surface has been in this state by examination of the largest craters. The 212 m diameter crater in figure 3C shows what is perhaps the most degraded of the large craters. Based on its morphology we could assume that this crater is so degraded that it is on the verge of being removed. Our above analysis shows that the time needed to remove a 212 m crater such as this is 13.8 Kyr, and given its degraded state this is likely to be only slightly more than the age of the crater itself. The largest crater in our sample (352 m, not shown) is partly infilled. Based on its diameter, the crater’s lifetime is expected to be 24.6 Kyr and so it must have formed more recently than this. This crater population contains no information related to epochs preceding this, thus the modeling of crater degradation we propose here will constrain environmental conditions 10-20 Kyr into the past.

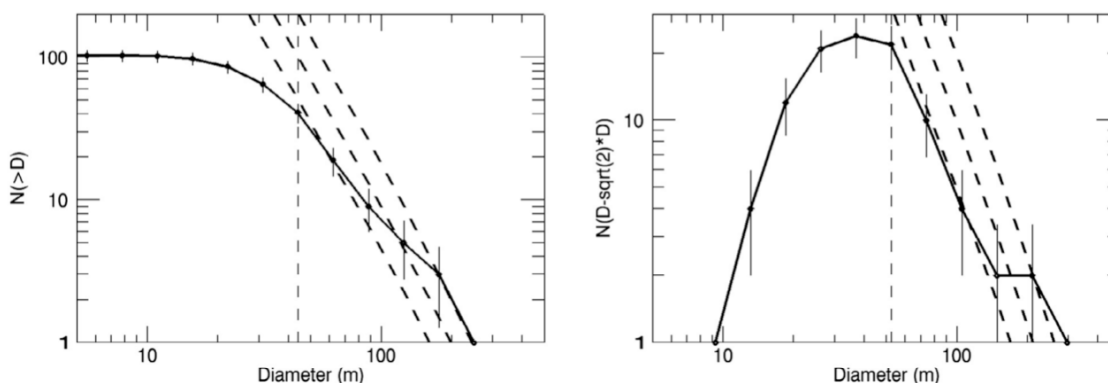


**Figure 5.** Cumulative (left) and differential (right) size-frequency distribution of craters in the ROI (Banks et al. 2010). Vertical dashed line shows diameter cutoff below which crater counts are incomplete. Inclined dashed lines represent the 5, 10, 20 Kyr isochrons (Hartmann, 2005).

We can also deduce the average accumulation rate within craters. Knowledge of initial crater depths would allow us to derive an accumulation rate as we know the time needed to fill

the crater. An estimate of the initial depth comes from a fresh 194 m crater (figure 3A) within our sample. This crater occurred in typical NPLD target material and is entirely fresh with a sharp rim and no accumulated interior ice. The depth to diameter ratio of this crater (from shadow lengths and a stereo DEM described below) is 0.26. If initial depth is  $0.26 * D$  for all these craters then dividing this by the expression for infilling time gives an accumulation rate of  $8.5 * D^{-0.14}$  mm/year (i.e. accumulation is slightly faster in smaller craters). Over the crater diameter range considered in our statistical analysis we derive the average accumulation rate within NPLD craters to be 4-5 mm/year.

The recent accumulation rate of the NPLD is unknown, however several studies [Laskar et al., 2002; Milkovich and Head, 2005; Milkovich et al., 2008] have argued for an accumulation rate close to 0.5 mm/year (an average over several 100 Kyr). The accumulation rate we derive for the interior of NPLD craters (an average over 10-20 Kyr) is an order of magnitude higher. This is not wholly unexpected as these craters appear to be preferential sites of accumulation today (figure 4) and this behavior is expected to persist into the past.

### 1.1.3 Additional Constraints from HiRISE stereo DEMs

This investigation is timely, as another new source of data has just become available. HiRISE stereo DEMs of three of the largest of these polar craters have been created and archived at the PDS by the HiRISE team. These DEMs have resolutions of 1m/pixel and vertical accuracies better than 1m. An example DEM covering one of our craters is shown as a perspective view in figure 6 below. In cases where shadows exist in the images (like this one), one can test the degree to which the DEMs accurately reproduce the shape of the surface of Mars. When shaded from the same direction, shadows in a shaded relief image should match the real shadow from the image in extent and shape. Figure 6 shows this to be the case for these polar DEMs.

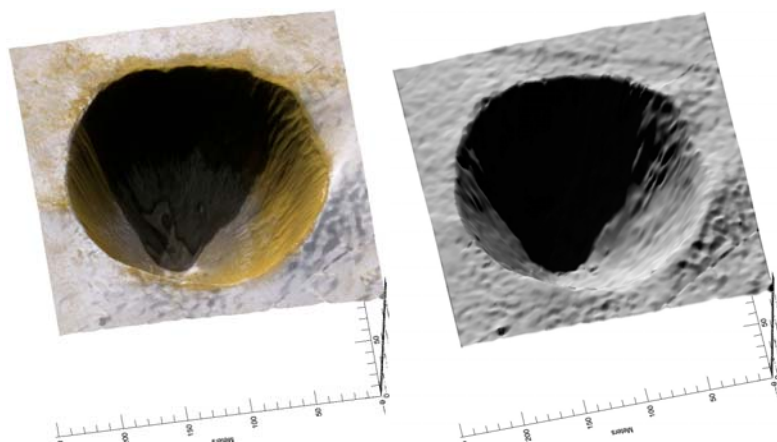


**Figure 6.** 3D perspective view of crater shown in figure 3A. HiRISE imagery (left) and shaded-relief illuminated from the same direction (right) are both draped over a HiRISE stereo DEM. The matching shadow shapes indicate that these DEMs are high-fidelity models of the shape of the real martian surface.

We will describe below how additional constraints can be extracted from the three DEMs of polar craters currently in the PDS created from HiRISE images:

- PSP\_001462\_2630+PSP\_001580\_2630 (our largest crater, diameter 350m, not shown)
- PSP\_009689\_2645+PSP\_010084\_2645 (a fresh crater, figure 3a)
- PSP\_009404\_2635+PSP\_010221\_2635 (a partly filled crater, figure 4a)

### 1.1.4 Proposal Objectives and Tasks

These crater-infilling rates are interesting, however the accumulation rate within craters is not the same as that of the surrounding landscape. In this proposal we will model the degradation and infilling of craters. The modeling will be constrained by the population statistics we just discussed and information gleaned from the stereo DEMs. The main parameter to solve

for is the atmospheric water content as a function of time (which drives condensation/sublimation of water ice). We will also investigate the formation of the meter-scale NRC texture shown in figure 1. Adaptation of published models describing suncups will allow us to back out the dustiness of the ice as described below. Once constrained, we will apply these same model conditions to the flat NRC surfaces to derive the accumulation rate of this terrain.

### Task 1: Incorporate new data into population statistics

In Banks et al. (2010), we reported on the positions and sizes of the NRC impact crater population. Due to incomplete HiRISE coverage in Mars Year 29, ~40% of the impact crater diameters were estimated from the CTX dataset. Now, HiRISE data from Mars year 30 covering these craters has been acquired and archived in the PDS.

*As an initial task to support the modeling tasks that follow, we propose to incorporate these more accurate diameter estimates into the analysis of Banks et al. An updated list of crater positions, diameters and degradation states will be created. We will archive this information with the PDS so future researchers interested in the NRC need not reinvent the wheel.*

We anticipate this will be a relatively short task that can be dealt with in year 1.

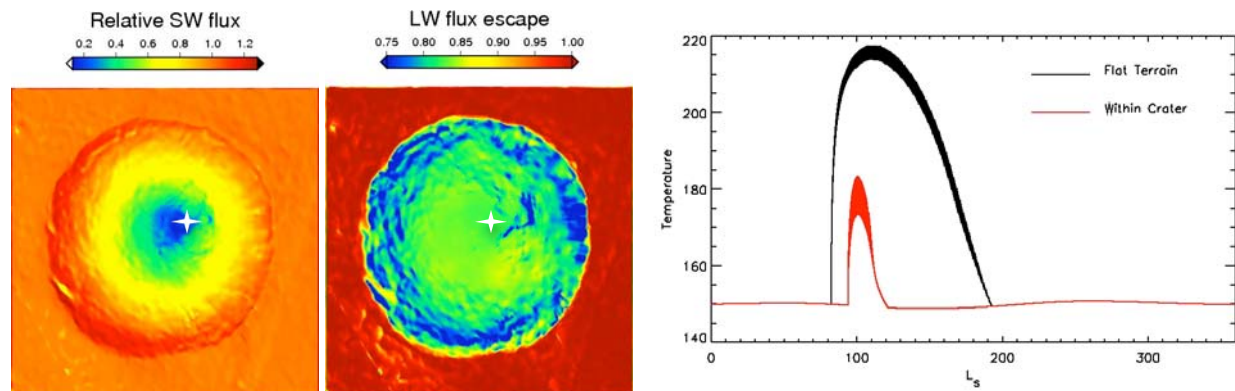


**Figure 7.** Geometric analysis of HiRISE stereo DEM of crater shown in Figure 3A. On the crater floor, the annual incident short-wave (SW) flux is dramatically reduced by shadowing while the annual emitted long-wave (LW) flux is only moderately reduced by the restricted portion of cold sky that is visible. White star marks location of example thermal model results shown. Fluxes are relative to flat unobstructed terrain. Width of temperature curves shows the diurnal variation.

### Task 2: Crater thermal model

In this task we will model the temperature history of terrain within craters over a range of latitudes suitable to the NRC (80-90 N). To do this we use the stereo-derived DEM of a fresh crater on the NRC shown in figure 6. This crater is close to the idealized simple-crater shapes parameterized by Melosh (1989). We will calculate slope and aspect at each point within the crater and run a thermal model through several years to establish the temperature history of a typical year at each point. Apart from the surface thermophysical properties, the boundary conditions of this thermal model at each timestep will be affected by:

- Direct insolation, thermal emission and shadowing
- Short- and long-wavelength scattered/emitted from adjacent terrain
- Short- and long-wavelength scattered/emitted from the atmosphere

On the floor of a crater such as this the cooling effect of shadowing competes with the warming effect of the restricted viewing angle to the cold sky. Which effect wins depends on the specific crater geometry and latitude in question. Figure 7 shows that in this case, where the



depth/diameter ratio is high (0.26) and the incidence angles are large, the shadowing effect easily beats the reduced-sky-area effect. A sample thermal mode run shows the crater floor is much colder than the exterior flat terrain and is the preferred site for ice accumulation when atmospheric humidity levels are high during the summer. Once fresh ice begins accumulating on the crater floor, it will be fine grained and have a high albedo (figure 4). This high albedo will drive further accumulation and fill the crater even when shadowing is no longer effective. We call the demonstration in figure 7 model\_0 i.e. it is a thermal model at a single point that incorporates only geometric effects on insolation, long-wavelength emission and shadowing.

*In this task, we will further develop model\_0 to be a thermal model of the whole DEM with more realistic boundary conditions. These improved boundary conditions will incorporate energy contributed by scattering and emission from the atmosphere and scattering from adjacent surface-elements e.g. crater walls.*

In previous work we have accounted for downwelling atmospheric radiation in two commonly used ways, either by reducing the surface emissivity or implementing a constant atmospheric radiation contribution equal to some fraction of the noon-time insolation. We propose to remove this relatively crude approximation by implementing the DISORT atmospheric scattering model (Stamnes et al. 1988), which uses a plane-parallel, multi-stream approach to solve for total downwelling radiation. DISORT is widely employed and has already been successfully used for Mars e.g. Wolff and Clancy (2003). Use of the companion model TWOSTR (based on DISORT and written by the same people) will also be investigated, as it is both faster and can handle spherical geometry (important for high-incidence angle situations).

We have experience incorporating surface scattering in modeling sublimation in landscapes on the south polar residual cap. This model incorporates scattering from adjacent terrain (e.g. Byrne and Ingersoll 2003; Byrne et al. 2008b). The south polar residual CO<sub>2</sub> cap is at one temperature at all points in the landscape. The north-polar situation is more complicated as energy in this water ice deposit is conducted in/out of the subsurface leading to temperatures that vary across the landscape and with time, which in turn leads to a complex scattering of long-wavelength radiation within the crater. We will integrate this scattering code with the model\_0.

In model\_0, we model conduction between subsurface layers with the usual approach of a finite difference scheme at a single point. We already used this model for examining sublimation of mid-latitude ice (Dundas and Byrne 2010; Byrne et al. 2009); example results are shown in figure 8. We will extend this model to run at each point within the crater DEM. Runs will last several martian years to stabilize the model after which we will extract an annual temperature history for each point within the crater.

All the models described here are written in the Interactive Data Language (IDL), which facilitates their integration. The challenge will be to optimize each model component so that runs can be concluded in reasonable amounts of time. The technical approach section describes some of these optimizations.

### **Task 3: Evolution of a single crater**

We will use this temperature history at each point in the DEM to calculate sublimation as we have done in recent work on mid-latitude ice deposits (Dundas and Byrne 2010; Byrne et al. 2009), see figure 8 for an example of previous work. We will repeat this process for many values of wind-speed and atmospheric water vapor; parameters to which forced and free convection are most sensitive (see technical methods section).

The available stereo DEMs provide constraints on sublimation of ice from the steep upper walls of the crater. Figure 9 shows horizontal slices through the DEM can be taken which

intersect the crater cavity. Circles can be fit to these intersections and the crater center retrieved. Higher (steeper) portions of the crater wall are shifted progressively more pole-ward. The skewed shape of the crater indicates the equatorward facing walls have been ablated ~5m more than the pole-facing walls. This is a key constraint, which our models must replicate. We will extract similar information from the other DEMs and adjust model parameters to replicate the degree of asymmetric expansion at the correct latitude and wall-slopes.

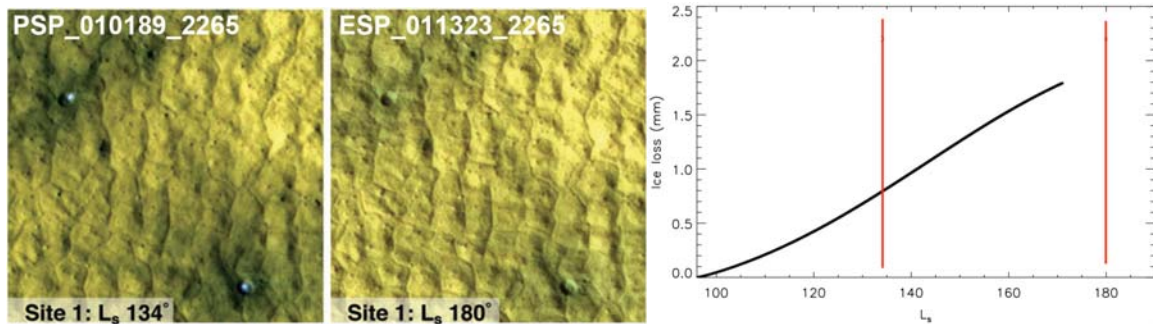


**Figure 8.** Example of previous work on modeling water ice sublimation and lag deposit accumulation. Mid-latitude ice exposed by two small impact craters is obscured by a sublimation lag in ~100 days (Byrne et al., 2009). Ice loss as a function of season (with image times indicated by red lines) is shown on the right (Dundas and Byrne, 2010).

This ablation of the crater walls results in a sublimation lag forming on these steep slopes. We will track the development of these lags in our model runs and allow this material to slump into the crater interior to cover up exposed ice on the shallow-sloping floor. Evidence for this ongoing process can be seen in figure 10, where it appears this lag has slumped measurably even within a single year. Mathematically, this can be accomplished by diffusion which is often used in numerical geomorphology to model downslope creep of debris e.g. Howard and Moore (2008) used such a scheme to model the creep of sublimation lags down the slopes of peaks on Callisto.

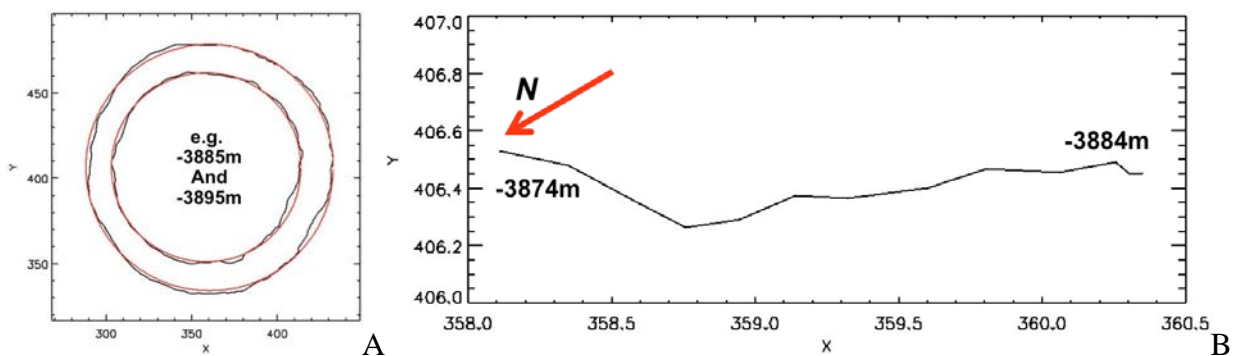


**Figure 9.** (A) Horizontal slices through the crater shown in figure 3A (black) can be fit by circles (red). (B) Derived crater-center position plotted as a function of elevation. Axes are in meters.

The effects of this process are twofold. Firstly, it will be to keep sublimation rates at the upper portions of the crater walls higher than they would otherwise be (by constantly removing the protective lag cover). Secondly, coating the icy floor of the crater with this low thermal-inertia material will encourage ice formation on the crater floor. One can see diffuse frost already forming on the dark material that has covered the floor of the crater in figure 3A. It's important to note that this lag material is volumetrically inconsequential. Accumulating ice and not debris

slumping from the walls ultimately fills the craters. Although minor in volume, this debris plays the important role of changing the thermophysical parameters of the surface.

*In task 3 we will model how a crater both expands in diameter due to asymmetric ablation (figure 9) and decrease in depth (as water ice is deposited in the initially shadowed crater floor). Changes in the shape of the crater will feedback into the calculation of thermal-history/sublimation-rates at each point as will accumulation and slumping of a sublimation lag (which will change the albedo and thermal properties of the material being modeled).* Thus, every few years we will recompute the temperatures and sublimation rates and evolve the shape and thermophysical properties of the crater accordingly. Each time this computation is performed we will also vary the insolation calculation to account for orbital changes (figure 2) over the 20 Kyr model run (orbital solutions available from Laskar et al. (2004)).

#### **Task 4: Accumulation and modification of crater populations over 20Kyr**

The production function of martian craters has recently been refined (Hartman 2005) and atmospheric screening of projectiles at small sizes has also been incorporated (Popova et al. 2003). Using this size-frequency distribution, we can generate a set of impact craters over the past 20Kyr to hit a region the size of our study area (as defined in section 1.1.2). This will give us a list of craters with their diameters and ages. Latitudes can be assigned randomly (although weighted for surface area at each latitude). We can be sure that the observed craters are primary impacts and not secondaries as no large (multi-kilometer) craters are known or suspected to have formed elsewhere on Mars to generate secondary impacts in this size range in the recent past. Abundant secondary craters ~100 m in diameter require a nearby primary crater at least 10 km diameter; a crater this size forms somewhere on Mars about every  $10^6$  yrs (Hartmann 2005), so it is unlikely that one formed close to the NPLD in the past  $\sim 10^4$  yrs. Furthermore, a field of secondary craters would have the same age and should be equally degraded and not have the widely variable preservation we observe.

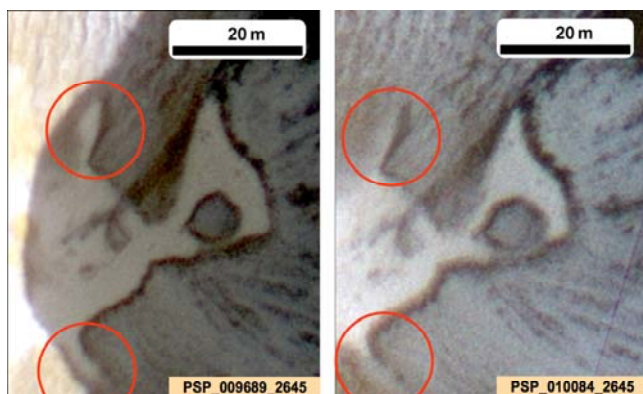


**Figure 10.** Evidence for downslope mass wasting on the crater floor (crater is shown in figure 3A). Viewing these images as a stereo-pair shows the dark material superposing the white, icy substrate. The dark material advanced over the floor of the crater in the circled areas over the course of about a month.

*We will use the model developed in the previous task to create populations of craters and evolve them forward in time. By matching the population statistics of our model population to that observed, we will solve for how atmospheric water vapor has varied over this period.* A crater will be considered removed when its depth decreases to some cutoff level (figure 3C shows craters can still be detected when almost completely full). We will investigate the effects of varying the value of this cutoff. Many of the craters will be removed entirely over the course of the model run; others will be degraded to varying degrees. We will compare the size-frequency statistics of our model population to that we have observed (figure 5) as a measure of how successful that particular set of model parameters was.

This task will be slow at first as we fully explore parameter space. However, after this initial phase we will be able to develop criteria where we know before running the full model that certain craters (e.g. very old and small ones) won't make it to the end of the modeled period and still be detectable. Once we refine these criteria, some craters in the simulated population can be deleted without needing to spend the time modeling their inevitable demise.

### Task 5: NRC suncup formation modeling

Examination of the right panel of figure 1 shows residual cap texture at the meter scale. Pervasive pits, ~1m across, form on the low darker areas (and in other locations also on the higher brighter areas). These pits closely resemble terrestrial suncups, which form through ablation of snow and ice fields in dry areas such as high-altitude glaciers. Scattering of light within a topographic hollow is scale-invariant i.e. you can rescale the feature while preserving its shape and the radiation incident on any point will not change. Suncups on the other hand have a well-defined scale that is set by the penetration of sunlight beneath the surface of the snow/ice. Sunlight 'diffuses' into these materials when photons scatter from ice-grain to ice-grain, the size of the suncups is related to how deeply this light can diffuse into the subsurface. Thus we can infer how deeply light penetrates into the upper decimeters of the NRC material by measuring suncup size and constructing a model to relate these two length-scales under martian conditions. How deeply light penetrates informs us about the dust content of the NRC material below the surface layer. This is independent information from the reflectance spectrum, which is dominated by light scattered from depths of less than one optical path length. The penetration of light into the subsurface is important to understand as it has implications for accurate thermal modeling (energy deposited at depth will result in lower surface temperatures/ablation).

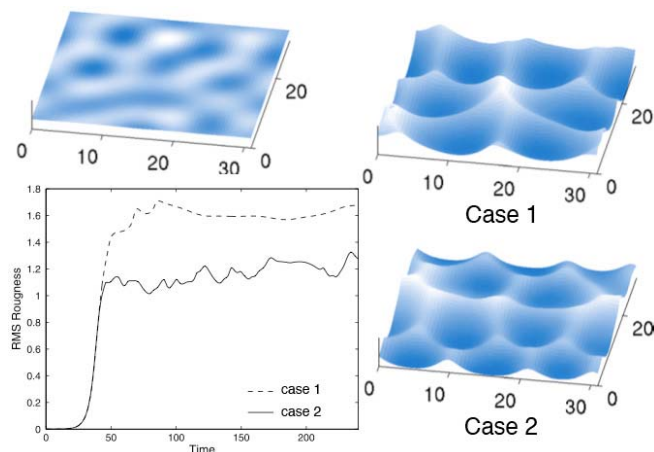


**Figure 11.** From figures 3 and 5 of Tiedje et al. (2006). Initial surface (colors indicate height) is shown in the upper left. Two final surfaces are shown on the right. Surface roughness vs. time is shown in the lower left (arbitrary time units), a statistical steady-state has been reached in both cases. Greater penetration of sunlight into the snow (case 1) produces larger, deeper suncups.

We will perform measurements of sun-cup size at a range of latitudes and elevations throughout the NRC. Models to relate suncup size to the penetration depth of sunlight already exist in the literature. This model is actually straightforward and works by combining penetration of light into the subsurface with curvature of the surface to produce a characteristic size of hollow that is stable while smaller and larger hollows are removed. Model results from Tiedje et al. (2006) can be seen in figure 11. We will utilize this basic model but make a suite of improvements. For instance Tiedje et al. assumed constant sunlight from directly overhead. Our work in task 2 will already allow us to calculate the actual orientation of incident light along with the contribution atmospheric scattering. Tiedje et al. also did not include thermal emission and assumed temperature was always constant.

*In task 5 we will model the development of the meter-scale surface texture. The result (sunlight penetration depths) will be related to the ice/dust ratio of the NRC. This task will allow us to investigate the dust deposition rate over the past few Kyr.*

### **Task 6: Application of results to the NPLD and extension to lower latitude craters**

Once our crater degradation models are constrained by the observed population statistics we will apply these same models to flat surfaces from 80-90N to produce a history of accumulation for the NPLD over the past 10-20 Kyr. The suncup modeling of these accumulating surfaces will allow us to constrain the dust-content of the upper decimeters.

The end result will be a self-consistent history of the upper few meters of the NPLD that incorporates and explains observations of the current crater population, surface textures, age and dust-content of the ice. The history retrieved will be a record of recent climate and provide the first link between orbital elements, climate, ice properties and polar stratigraphy.

Several lower-latitude craters (well-separated from the NPLD) contain high-albedo ice deposits. We will also apply our models and derived climate histories to these deposits to investigate their origin and current mass-balance. Two craters of special interest are Korolev (73N) and Louth (70N) (see Armstrong et al. 2005 and Brown et al. 2008 for descriptions) as they are both far from the NRC yet have similar surface textures.

Water vapor histories derived over the NRC will be generalized to nearby non-polar locations by using atmospheric eddy mixing such as that done to track argon enrichments and mixing in today's atmosphere (Sprague et al. 2004, 2007).

## **1.2 Technical Approach and Methodology**

### **1.2.1 Task 1: Update population statistics**

We will assemble all data in a geographic information system (we use ArcGIS by ESRI). A table of crater location, size, degradation state and depth to diameter ratio (if available) will be created and archived at the PDS. Additionally, we will check historical THEMIS VIS, MOC and Viking imagery to see if it is possible to constrain the formation date of any of these craters. In the case of Viking, this check can only be done for the largest craters. An initial check for the crater in figure 3a shows that it existed in Viking images (as a single dark pixel) 32 years ago.

The technical details of how to update the interpretation of the population statistics using the better, HiRISE-only, diameters are recounted in section 1.1.2 and Banks et al. (2010).

### **1.2.2 Task 2: Crater thermal model**

In this task we will combine models that are both new and some that have been previously created by us for other Mars research. We calculate insolation by using the NAIF SPICE library to return solar distance as a function of time. Incidence angle for flat terrain is given by:

$$\cos(i_f) = \sin(\text{latitude})\sin(\text{dec}) + \cos(\text{latitude})\cos(\text{dec})\cos(\text{hour angle})$$

$$\text{where: } \text{dec} = \sin^{-1}(\sin(\text{Obliquity})\sin(L_s))$$

Incidence angle for terrain with a slope 's' and aspect 'a' are given by:

$$\cos(i_s) = \cos(i_f)\cos(s) + \sin(i_f)\sin(s)\cos(\Delta A) \quad \text{where} \quad \Delta A = \left| a - \cos^{-1}\left(\frac{\sin(\text{dec}) - \sin(\text{lat})\cos(i_f)}{\cos(\text{lat})\sin(i_f)}\right) \right|$$

Shadowing is calculated with simple geometric tests of the angular height of topography as seen by the point of interest. No correction for planetary curvature or the martian geoid is needed as these DEMs cover very small areas.

We will experiment with two approaches to calculate the scattered radiation at each point from the surrounding surface. The first method was pioneered by Vasavada et al. (1999) for

Lunar and Mercurian craters. The flux leaving a surface element ( $F_j$ ) is albedo times the incident flux, which is the sum of direct sunlight and the some portion ( $\alpha$ ) of the flux leaving all the other surface elements. This portion of flux scattered from element  $i$  to  $j$  depends on the angles their surface normals make to the line that connects them ( $\theta_i$  and  $\theta_j$ ) and their separation ( $d_{ij}$ ):

$$F_j = A_j \left( \sum_{i=1}^N F_i \alpha_{ij} + S_o \cos(i_s) \right) \quad \text{where} \quad \alpha_{ij} = \frac{\cos(\theta_i) \cos(\theta_j)}{\pi d_{ij}^2}$$

The absorbed flux is  $F_j(1-A_j)/A_j$  where  $A_j$  is the albedo of the surface element. This sets up a linear system of equations that can be solved using standard linear algebra packages. A similar set of equations can be constructed for thermal emission and scattering of long-wavelength radiation. The problem is that the number of equations ( $N$ ) equals the number of surface elements and this needs to be solved every model timestep. We will use a reduced resolution DEM when calculating surface scattering to keep  $N$  low and model run times reasonable.

The alternative approach is to represent the crater as a cylindrically symmetric set of bands such as we have done in the past (Byrne and Ingersoll, 2003). Although the equations are more complex, the solution is much faster as only a limited number of surface elements are needed to represent the crater. This model also requires that insolation be azimuthally symmetric (i.e. it can only be used at the pole) so no investigations of the effect of latitude or crater asymmetries can be carried out. This symmetry also means that local-time is no longer important and one need only use just a few hundred timesteps per year which further speeds things up.

We will use the publicly available DISORT and TWOSTR models ([ftp://climate1.gsfc.nasa.gov/wiscombe/Multiple\\_Scatt/](ftp://climate1.gsfc.nasa.gov/wiscombe/Multiple_Scatt/)) to improve our quantification of the downwelling atmospheric radiation. DISORT is a multistream model whereas TWOSTR is limited to a two-stream solution. Its advantage lies in that it can handle spherical geometry whereas DISORT uses the plane-parallel approximation, which might become a problem in the polar regions where incidence angles are always high. We will test these models against each other for the two-stream solution to see how the plane-parallel DISORT performs. If the plane-parallel assumption is not too serious (<5% difference) we will use DISORT in multistream mode, otherwise we will use TWOSTR. These models can be constrained by the atmospheric temperature measurements of the Mars Climate Sounder (MCS) instrument (from heights of 0-80km) taken the north polar summer of Mars Year 29 (2008 on Earth's Calendar). We will also use Thermal Emission Spectrometer (TES) measurements of the atmospheric opacity and temperature, over locations on the NRC. These measurements are available every day for several, years (Smith, 2008). Local-time coverage is poor; however, diurnal variation of atmospheric temperature and opacity in these near-polar locations is likely to be small.

### 1.2.3 Task 3: Evolution of a single crater

The sub-surface heat diffusion approach to thermal modeling has been widely used for decades and the formulas won't be reproduced here. See Dundas and Byrne (2010) for our most recent implementation of this model. We use a fully explicit solution and employ the Courant criteria to choose the timestep length and so maintain numerical stability. Sublimation is calculated as the sum of free and forced convection:

$$m_{forced} = M_w \frac{1}{kT} A u_{wind} (e_{sat} - e) \quad \text{and} \quad m_{free} = 0.14 \Delta \eta \rho_{ave} D \left( \left( \frac{\Delta \rho}{\rho} \right) \left( \frac{g}{v^2} \right) \left( \frac{v}{D} \right) \right)^{\frac{1}{3}}$$

Our free-convection equation is closely related to that derived by Ingersoll (1970) and a similar expression from Hecht (2002), while forced convection follows that derived by Paterson (1994) and Ivanov and Muhleman (2000). We include latent heat effects in the surface energy balance

of the thermal model. The diffusion coefficient  $D$  and kinematic viscosity  $\nu$  are calculated using equations from Chittenden et al. (2008). The buoyancy term  $\Delta\rho/\rho$  comes from Mills (2001) and accounts for thermal as well as compositional effects on buoyancy. We will vary wind-speed ( $u_{wind}$ ) and atmospheric water vapor partial pressure ( $e$ , which along with temperature also controls the  $\Delta\eta$  term) to find the best match between modeled and observed crater populations.

The downslope movement of debris is often approximated by linear diffusion with a constant diffusivity; however, it is now known (from terrestrial experience) that the diffusivity over high slopes should be slope-dependent so that the diffusion itself is non-

$$\frac{\partial z}{\partial t} = -\nabla \cdot \left[ D_1 \nabla z + D_2 \left( \frac{\left\{ |\nabla z|/S \right\}^x}{1 - \left\{ |\nabla z|/S \right\}^x} \right) \widetilde{\nabla z} \right]$$

linear (Roering et al. 1999) i.e. mass-wasting should evolve the topography according to the formula above, where  $S$  is the critical slope at which the mass-wasting rate is infinitely large and  $D_1$ ,  $D_2$  &  $x$  are constants that control the diffusivity (and  $\nabla z = |\nabla z| \widetilde{\nabla z}$ ). In the limit of small slopes ( $|\nabla z| \ll S$ ) this reduces to the commonly-used linear diffusion. By incorporating this effect we can redistribute a lag-deposit formed on high slopes downhill.

Such non-linear diffusion has been previously applied to modeling of the degradation of martian craters (Forsberg-Taylor et al. 2004; Howard, 2007). Our situation differs somewhat as the volume of this material is insignificant compared to the craters. This mass-wasted material is not filling in the crater; it covers the icy floor allowing ice to beginning accumulating there. The craters are filled by ice accumulating on top of the lag deposit and not by the lag deposit itself.

**1.2.4 Task 4: Accumulation and modification of crater populations over 20Kyr**

This task involves running the previously described model many times. See sections 1.2.2 and 1.2.3 for technical description of the models. Populations of craters can be generated from the cratering rate estimates of Hartmann (2005).

**1.2.5 Task 5: NRC suncup formation modeling**

The model of Tiedje et al (2006) is described in detail in their paper and the equations are quite lengthy. In their model, the change in an input height field ( $h$ ) can be evaluating by combining  $\nabla^2 h$  and  $\nabla^4 h$  linearly. The former term causes instabilities to grow and dominates at short wavelengths whereas the latter term damps instabilities and dominates at longer wavelengths. The result is that instabilities (suncups) grow to a certain size, but not larger. The coefficients of this linear combination of terms depend on the penetration depth of sunlight into the ice and so the equilibrium suncup size is linked to this parameter.

The weaknesses in their model are discussed in the description of task 5 above. It will be necessary for us to re-derive their model with more realistic geometries. In addition, they made their analysis non-dimensional whereas we wish to keep track of real quantities and timescales.

**1.2.6 Task 6: Application of results to the NPLD and extension to lower latitude craters**

This task involves combining model results from the previous tasks. The technical details of how these models run are recounted in the previous subsections.

**1.3 Expected significance and relevance to NASA goals**

This work is relevant to the goals of the **Mars Data Analysis Program** whose objective is to enhance the scientific return from missions to Mars. Through analysis of CTX and HiRISE images and HiRISE stereo DEMs we will be able to elucidate the recent climate history and polar resurfacing of Mars. By extracting fresh scientific understanding from these mission data the proposed work is relevant to MDAP.

We also address an area designated as high-priority to MDAP that support future missions: “*Analysis and comparison of Mars orbital and surface data to increase the predictive accuracy of surface characteristics of Mars from orbit*”. Though this work we will further our understanding of the surface conditions on the north polar cap, which has been proposed in the past as a destination for Chronos and Boreale Explorer (scout proposals) and which will likely be visited by landed craft in the future.

Community-wide consensus of which research goals and objectives are most important to further understanding of Mars is summarized in the 2008 **MEPAG report**. This investigation bears directly on goal II of that report, understanding the Martian climate: “*Understand how volatiles and dust exchange between surface and atmospheric reservoirs, including the mass and energy balance. Determine how this exchange has affected the present distribution of surface and subsurface ice as well as the Polar Layered Deposits (PLD)*.”.

This proposal also directly addresses **NASA strategic sub-goal 3C** (NASA, 2006): “*Advance scientific knowledge of the origin and history of the solar system, the potential for life elsewhere, and the hazards and resources present as humans explore space.*”, by deriving the recent history of the solar system body Mars.

**1.4 Work Plan and Team Roles**

We plan to present our results both at annual conferences and in the published literature.

YR	Task	Personnel
1	Task 2: Model Development – thermal model and surface scattering	Byrne, Russell
	Task 2: Model Development – Atmospheric radiation I	Russell
	Task 1: Update population statistics with new data, archive at PDS.	Student
2	Task 3: Model Development–mass wasting & crater expansion	Byrne
	Task 2: Model Development – Atmospheric radiation II	Russell
	Task 5: Suncup measurements, adaptation of Tiedje et al. (2006)	Student
3	Tasks 2 and 3: Integration of model components – optimize runtimes	Byrne/Russell
	Task 5: Conclude suncup model development and produce results	Student
	Task 4: Create and modify model crater populations I	Student
4	Task 4: Create and modify model crater populations II	Student
	Task 6: Application of results to flat areas of the NRC	All
	Task 6: Application of results to the lower latitude craters	All

**Principle Investigator (0.167 FTE):** Professor Shane Byrne (Lunar and Planetary Lab) will be responsible for the implementation of this proposal. He will develop the surface-scattering and mass-wasting models and will be involved continuously in interpretation of the results. He will advise the graduate student, training them to complete their tasks.

**Co-Investigator (0.1 FTE):** Dr. Patrick Russell (Smithsonian Institute) is experienced in image analysis, quantitative photometric modeling of HiRISE data and modeling sublimation of ice within craters. He will lead incorporation of atmospheric radiation scattering and contribute to other model components especially surface scattering.

**Graduate Student (1.0 FTE):** A graduate student (Lunar and Planetary Lab) will perform the analysis tasks using the models outlined in this proposal and further developed by Dr.s Byrne and Russell. The student in question is expected to start in the summer of 2011.



## 2. References

- Armstrong, J.C., T.N. Titus and H.H. Kieffer (2005), Evidence for subsurface water ice in Korolev crater, Mars, *Icarus*, 174(2), 360-372.
- Banks, M.E., S. Byrne, K. Galla, A.S. McEwen, V.J. Bray, K.E. Fishbaugh, C.M. Dundas, K.E. Herkenhoff, B.C. Murray and the HiRISE Team (2010), Crater Population and Resurfacing of the Martian North Polar Layered Deposits, *J. Geophys. Res.*, 115, E08006.
- Brown, A., S. Byrne, L.L. Tornabene and T. Roush (2008), Louth crater: Evolution of a layered water ice mound, *Icarus*, 196(2), 433-445.
- Byrne, S., A.P. Ingersoll (2003). A Sublimation Model for Martian South Polar Ice Features. *Science* 299: 1051-1053.
- Byrne, S., M.T. Zuber and G.A. Neumann (2008a), Interannual and seasonal behavior of Martian residual ice-cap albedo, *Planet. Space Sci.*, 54, 2,194-211.
- Byrne, S., P. S. Russell, K. E. Fishbaugh, C. J. Hansen, K. E. Herkenhoff, A. S. McEwen, and the HiRISE Team (2008b), Explaining the Persistence of the Southern Residual Cap of Mars: HiRISE Data and Landscape Evolution Models, *LPSC 39*, 2252.
- Byrne, S. (2009), The polar deposits of Mars, *Annual Review of Earth Planetary Science*, 37.
- Byrne, S., and 17 colleagues (2009), Distribution of Mid-Latitude Ground-Ice on Mars from New Impact Craters, *Science*, 325, 1674, 2009.
- Chamberlain, M.A., and W.V. Boynton (2007). Response of Martian ground ice to orbit-induced climate change. *J. Geophys. Res.* 112, E06009.
- Chittenden, J. D., Chevrier, V., Roe, L. A., Bryson, K., Pilgrim, R., Sears, D. W. G., 2008. Experimental study of the effects of wind on the stability of water ice on Mars. *Icarus* 196, 477-487.
- Dundas, C.M., and S. Byrne, Modeling Sublimation of Ice Exposed by Recent Impacts in the Martian Mid-Latitudes, *Icarus*, 206(2), 716-728, 2010.
- Fishbaugh KE, Hvidberg CS, Beaty D, Clifford S, Fisher D, et al. (2008). Introduction to the 4th Mars Polar Science and Exploration Conference special issue: Five top questions in Mars polar *Science. Icarus* 196: 305-317.
- Forsberg-Taylor, N. K., A. D. Howard, and R. A. Craddock (2004), Crater degradation in the Martian highlands: Morphometric analysis of the Sinus Sabaeus region and simulation modeling suggest fluvial processes, *J. Geophys. Res.*, 109, 5002.
- Hale, A.S., D.B. Bass and L.K. Tamppari (2005). Monitoring the perennial martian northern polar cap with MGS MOC. *Icarus* 174: 502-512
- Hartmann, W.K. (2005), Martian cratering 8: Isochron refinement and the chronology of Mars, *Icarus*, 174, 294-320.
- Hecht, M. H., 2002. Metastability of liquid water on Mars. *Icarus* 156, 373-386.
- Herkenhoff KE, Byrne S, Russell PS, Fishbaugh KE, McEwen AS. (2007). Meter-Scale Morphology of the North Polar Region of Mars. *Science* 317: 1711.

- Herkenhoff KE, Plaut JJ. 2000. Surface Ages and Resurfacing Rates of the Polar Layered Deposits on Mars. *Icarus* 144: 243-253.
- Howard, A. D. (2007), Simulating the development of Martian highland landscapes through the interaction of impact cratering, fluvial erosion, and variable hydrologic forcing, *Geomorphology*, 91, 332-363.
- Howard, A.D. and J.M. Moore (2008), Sublimation-driven erosion on Callisto: A landform simulation model test, 35(3), L03203.
- Ingersoll, A. P., 1970. Mars: Occurrence of liquid water. *Science* 168, 972-973.
- Ivanov, A. B., and D. O. Muhleman (2000), The role of sublimation for the formation of the northern ice cap: Results from the Mars Orbiter Laser Altimeter, *Icarus*, 144, 436-448.
- Kieffer, H. H., 1990. H<sub>2</sub>O grain size and the amount of dust in Mars' residual north polar cap. *J. Geophys. Res.* 95, 1481-1493.
- Kreslavsky, M.A. (2009), Dynamic landscapes at high latitudes on Mars: Constraints from populations of small craters, *Lunar Planet. Sci. Conf.*, XXXX, 2311.
- Langevin, Y., F. Poulet, J. P. Bibring, B. Schmitt, S. Doute, and B. Gondet (2005), Summer evolution of the north polar cap of Mars as observed by OMEGA/Mars Express, *Science*, 307, 1581, DOI: 10.1126/science.1109438.
- Laskar, J. A., A. C. M. Correia, M. Gastineau, F. Joutel, B. Levrard, and P. Robutel (2004), Long term evolution and chaotic diffusion of the insolation quantities of Mars, *Icarus*, 170, 2, 343-364.
- Laskar J., B. Levrard, and J. F. Mustard (2002), Orbital forcing of the Martian polar layered deposits, *Nature*, 419, 375-77.
- Levrard B, Forget F, Montmessin F, Laskar J. 2007. Recent formation and evolution of northern Martian polar layered deposits as inferred from a Global Climate Model. *J. Geophys. Res.* 112: 6012.
- Malin MC, Edgett KS. 2001. Mars Global Surveyor Mars Orbiter Camera: Interplanetary cruise through primary mission. *J. Geophys. Res.* 106: 23429-23570.
- McCleese, D.J., and 18 colleagues (2008), Intense polar temperature inversion in the middle atmosphere on Mars, *Nature Geoscience*, 1, 745-749.
- Melosh, H. J., 1989. Impact Cratering: A Geologic Process. Oxford University Press, New York.
- Milkovich, S. M., and J. W. Head III (2005), North polar cap of Mars: Polar layered deposit characterization and identification of a fundamental climate signal, *J. Geophys. Res.*, 110, 1005.
- Milkovich, S. M., J. W. Head, G. Neukum, and the HRSC Team (2008), Stratigraphic analysis of the northern polar layered deposits of Mars: Implications for recent climate history, *Planet. Space Sci.*, 56, 266-88.
- Montmessin, F., R. M. Haberle, F. Forget, Y. Langevin, R. T. Clancy, and J.-P. Bibring (2007), On the origin of perennial water ice at the south pole of Mars: A precession-controlled mechanism?, *J. Geophys. Res.*, 112 (E08S17).

- Mills, A. F. 2001. *Mass Transfer*. Prentice Hall, New Jersey.
- Paterson, W. S. B., 1994. *The Physics of Glaciers*, 3<sup>rd</sup> Ed. Butterworth Heinemann, Oxford.
- Perron, J.T., J.W. Kirchner and W.E. Dietrich (2008), Spectral signatures of characteristic spatial scales and nonfractal structure in landscapes, *J. Geophys. Res.*, 113, F04003.
- Perron, J.T., and P. Huybers (2009), Is there an orbital signal in the polar layered deposits on Mars?, *Geology*, 37(2), 155-159.
- Phillips RJ, Zuber MT, Smrekar SE, Mellon MT, Head JW, et al. 2008. Mars North Polar Deposits: Stratigraphy, Age, and Geodynamical Response. *Science* 320: 1182.
- Popova, O., I. Nemtchinov, and W. K. Hartmann (2003), Bolides in the present and past Martian atmosphere and effects on cratering processes, *Meteorit. Planet. Sci.*, 38, 905–925.
- Roering, J.J., Kirchner, J.W., Dietrich, W.E., 1999. Evidence for nonlinear, diffusive sediment transport on hillslopes and implications for landscape morphology. *Water Resources Research* 35 (3), 853–870.
- Schorghofer N. 2007. Dynamics of ice ages on Mars. *Nature* 449: 192-194.
- Sprague, A. L., W. V. Boynton, K. E. Kerry, D. M. Janes, D. M. Hunten, K. J. Kim, R. C. Reedy, and A. E. Metzger (2004), Mars' South Polar Ar Enhancement: A Tracer for South Polar Seasonal Meridional Mixing, *Science*, 306, 1364-1367.
- Sprague, A. L., W. V. Boynton, K. E. Kerry, D. M. Janes, N. J. Kelly, M. K. Crombie, S. M. Melli, J. R. Murphy, R. C. Reedy, and A. E. Metzger (2007), Mars' atmospheric argon: Tracer for understanding Martian atmospheric circulation and dynamics, *J. Geophys. Res.*, 112.
- Smith, M.E. (2008), Spacecraft Observations of the Martian Atmosphere, *Annual Review of Earth Planetary Science*, 36.
- Stamnes K, Tsay SC, Wiscombe W, Jayaweera K. 1988. Numerically stable algorithm for discrete-ordinate-method radiative transfer in multiple scattering and emitting layered media. *Appl. Opt.* 27: 2502–2509.
- Tanaka K. L. (2005), Geology and insolation-driven climatic history of Amazonian north polar materials on Mars, *Nature*, 437, 991-994.
- Thomas PC, Malin MC, Edgett KS, Carr MH, Hartmann WK, et al. 2000. North-south geological differences between the residual polar caps on Mars. *Nature* 404: 161-164.
- Tiedje, T., K.A. Mitchell, B. Lau, A. Ballestad and E. Nodwell (2006), Radiation transport model for ablation hollows on snowfields, *J. Geophys. Res.*, 111, F02015.
- Titus TN, Calvin WM, Kieffer HH, Langevin Y, Prettyman TH. 2008. Martian Polar Processes, In *The Martian Surface: Composition, Mineralogy, and Physical Properties*, ed. JF Bell III, 25, Cambridge University Press.
- Vasavada, A. R., D. A. Paige, and S. E. Wood 1999. Near-Surface Temperatures on Mercury and the Moon and the Stability of Polar Ice Deposits. *Icarus* 141, 179-193.
- Wolff MJ, Clancy RT. 2003. Constraints on the size of Martian aerosols from Thermal Emission Spectrometer observations. *J. Geophys. Res.* 108: 5097.

### 3. Facilities and equipment

The considerable volume of the available datasets for the Martian polar regions poses a challenge. The arrival of the HiRISE dataset, where a handful of images can exceed the entire Viking camera dataset in terms of number of pixels, brings this issue into sharp focus. Analysis of these data needs extensive computational resources that previously would have been considered luxury items.

Here at the Lunar and Planetary Laboratory we are fortunate to have immediate access to the HiRISE dataset, which is stored locally. All processed (including projected and color products) and raw HiRISE products are accessible to us through the local network. A wide variety of software packages relevant to this work are available through the university/department site license such as IDL/ENVI, Matlab, ISIS, ArcGIS, GMT as well as figure and manuscript preparation software such as Adobe Photoshop and Illustrator along with Microsoft office.

The PI has a multi-processor desktop with an associated raid array that can be used to complete the model development tasks outlined for him in this proposal. The PI is director of the Space Imagery Center here at the Lunar and Planetary Laboratory, which is one of the NASA RPIF (Regional Planetary Image Facilities) centers. This facility holds archives of previous spacecraft missions to the Moon, Mars and other planets and employs a full time lab manager. As an RPIF, the resources of the imagery center are at the disposal of all planetary science researchers. We have recently invested in a 12TB disk system that will store lunar and martian datasets.

#### 4. Curricula Vitae

<b>Shane Byrne</b> <b>Assistant Professor</b>	<b>Department of Planetary Sciences</b> <b>University of Arizona</b>
<b>Mail:</b> Lunar and Planetary Laboratory, The University of Arizona, 1629 E. University Blvd., Tucson, AZ 85721-0092, USA.	<b>Phone:</b> (520) 626-0407 <b>Fax:</b> (520) 621-4933 <b>Email:</b> shane@lpl.arizona.edu <b>http://www.lpl.arizona.edu/~shane</b>

#### Professional Positions

- University of Arizona – Lunar and Planetary Laboratory, 8/2007 - Present**  
Assistant Professor  
Director: Space Imagery Center–A NASA Regional Planetary Image Facility
- University of Arizona – Lunar and Planetary Laboratory, 9/2005 – 8/2007.**  
Research Associate – with HiRISE team.
- Massachusetts Institute of Technology, 12/2003 – 9/2005.**  
Postdoctoral Scholar – with Professor Maria Zuber.
- California Institute of Technology, 6/2003 – 12/2003.**  
Assistant Scientist – with Professor Bruce Murray.
- California Institute of Technology, 8/1998 – 6/2003.**  
Graduate Research Assistant – with Professors Murray and Ingersoll.

#### Education

- California Institute of Technology, Pasadena, CA. 1998-2003**  
Ph.D. Planetary Science, with minor in Astronomy (2003)  
Advisors: Professors Bruce C. Murray and Andrew P. Ingersoll
- M.S. Planetary Science, with minor in Astronomy (2001)
- University of Cardiff, Cardiff, United Kingdom 1994-1998**  
Master of Physics. Astrophysics (1998)

#### Planetary Mission Involvement

- High-Resolution Stereo Color Imager (HiSCI) – Deputy-PI.
- High Resolution Science Experiment (HiRISE) – Co-Investigator.
- Chronos Mars-scout proposal (2006) – Co-Investigator.
- MOSAIC Mars-scout proposal (2006) – Co-Investigator.
- Boreale Explorer Mars-scout proposal (2006) – Co-Investigator.
- Mars Orbiter Laser Altimeter (MOLA) (2002-2006).
- MIT manned lunar exploration initiative (2004-2005).
- Landing site selection, Mars Polar Lander (1999).

#### Service and Professional Memberships

- Session Chair: American Geophysical Union – Fall Meeting  
International conference on Mars polar science and exploration  
Lunar and Planetary Science Conference
- Reviewer: NASA review panels, Nature, Science, Journal of Geophysical Research, Geophysical Research Letters, Icarus, Planetary and Space Science, The Mars Journal, Annals of Glaciology.
- Member: American Geophysical Union  
American Astronomical Society – Division of Planetary Science

**Selected Publications**

- Diniega, S., **S. Byrne**, N.T. Bridges, C.M. Dundas and A.S. McEwen, Seasonality of Present-day Martian Dune-Gully Activity, *Geology*, In Press, 2010.
- Sharma, P., and **S. Byrne**, Constraints on Titan's topography through fractal analysis of shorelines, *Icarus*, In Press, 2010.
- Banks, M.E., **S. Byrne**, K. Galla, A.S. McEwen, V.J. Bray, K.E. Fishbaugh, C.M. Dundas, K.E. Herkenhoff, B.C. Murray and the HiRISE Team, Crater Population and Resurfacing of the Martian North Polar Layered Deposits, *J. Geophys. Res.*, 115, E08006, 2010.
- Reufer, A., N. Thomas, W. Benz, **S. Byrne**, V. Bray, C. Dundas and M. Searls, Models of high velocity impacts into dust-covered ice: Application to Martian northern lowlands, *Planet. Space Sci.*, 58(10), 2010.
- Diniega, S., K. Glasner and **S. Byrne**, Long-time evolution of models of aeolian sand dune fields: Influence of dune formation and collision, *Geomorphology*, 121, 55-68, 2010.
- Holt, J.W., K.E. Fishbaugh, **S. Byrne**, S. Christian, K. Tanaka, P. S. Russell, K.E. Herkenhoff, A. Safaenili, N.E. Putzig, and R.J. Phillips, The Construction of Chasma Boreale on Mars, *Nature*, 465, 446-449, 2010.
- Dundas, C.M., A.S. McEwen, S. Diniega, and **S. Byrne**, New and recent gully activity on Mars as seen by HiRISE, *Geophys. Res. Lett.*, 37(7), L07202, 2010.
- Dundas, C.M., and **S. Byrne**, Modeling Sublimation of Ice Exposed by Recent Impacts in the Martian Mid-Latitudes, *Icarus*, 206(2), 716-728, 2010.
- Hansen, C.J., N. Thomas, G. Portyankina, A. McEwen, T. Becker, **S. Byrne**, K. Herkenhoff, H. Kieffer, M. Mellon, HiRISE Observations of gas sublimation-driven activity in Mars' southern polar regions: I. Erosion of the Surface, *Icarus*, 205(1), 283-295, 2010.
- Byrne, S.**, and 17 colleagues, Distribution of Mid-Latitude Ground-Ice on Mars from New Impact Craters, *Science*, 325, 1674, 2009.
- Byrne, S.**, The polar deposits of Mars, *Ann. Rev. Earth Plan. Sci.*, 37, 2009.
- Russell, P., and 10 colleagues, Seasonally active frost-dust avalanches on a north polar scarp of Mars captured by HiRISE, *Geo. Phys. Lett.*, 35(23), L23204, 2008.
- Brown, A., **S. Byrne**, L.L. Tornabene and T. Roush, Louth crater: Evolution of a layered water ice mound, *Icarus*, 196(2), 433-445, 2008.
- Winebrenner, D.P., M.R. Koutnik, E.D. Waddington, A.V. Pathare, B.C. Murray, **S. Byrne** and J.L. Bamber, Evidence for ice flow prior to trough formation in the martian north polar layered deposits, *Icarus*, 195(1), 90-105, 2008.
- Byrne, S.**, M. T. Zuber, G. A. Neumann, Interannual and Seasonal Behavior of Martian Residual Ice-Cap Albedo, *Planet. Space Sci.*, 56(2), 194-211, 2008.
- Herkenhoff, K.E., **S. Byrne**, P.S. Russell, K.E. Fishbaugh, and A.S. McEwen, HiRISE Observations of the North Polar Region of Mars, *Science*, 317, 1711, 2007.
- Koutnik, M., **S. Byrne**, B.C. Murray, A.D. Toigo, and Z.A. Crawford, Eolian Controlled Modification of the Martian South Polar Layered Deposits, *Icarus*, 174, 490-501, 2005.
- Schaller, E.S., B.C. Murray, A.V. Pathare, J. Rasmussen, and **S. Byrne**, Modification of Secondary Craters on the Martian South Polar Layered Deposits, *J. Geophys. Res.*, 31, L21701, 2005.
- Byrne, S.**, and A.B. Ivanov, The Internal Structure of the Martian South Polar Layered Deposits, *J. Geophys. Res.*, 109, E11001, 2004.
- Jerolmack, D., D. Mohrig, M.T. Zuber, and **S. Byrne**, A minimum time for the formation of the Holden Northeast Fan, Mars, *Geophys. Res. Lett.*, 31, L21701, 2004.
- Piqueux, S., **S. Byrne**, and M.I. Richardson, The sublimation of Mars southern CO<sub>2</sub> ice cap and the formation of "spiders", *J. Geophys. Res.*, 108(E8), 2003.
- Byrne, S.**, and A.P. Ingersoll, Martian climatic events on timescales of centuries: Evidence from feature morphology in the residual south polar cap, *Geophys. Res. Lett.*, 30(13), 2003.
- Byrne, S.**, and A.P. Ingersoll, A Sublimation Model for Martian South Polar Ice Features, *Science*, 299, 1051-1053, 2003.
- Koutnik, M., **S. Byrne**, and B.C. Murray, South Polar Layered Deposits of Mars: The Cratering Record, *J. Geophys. Res.*, 107(E11), 5100, 2002.
- Byrne, S.**, and B.C. Murray, North polar stratigraphy and the paleo-erg of Mars, *J. Geophys. Res.*, 107(E6), 2002.

**Patrick Russell (CO-I)**

- Center for Earth and Planetary Studies, National Air and Space Museum, Smithsonian Institution
- MRC 315 PO Box 37012 Washington DC 20013-7012 Ph: 202-633-2487 Email: russellp@si.edu
  - **Professional Experience**
    - Research Physical Scientist, Center for Earth & Planetary Studies, Smithsonian Institution, 2009-pres.
    - Team member, High Resolution Imaging Science Experiment on NASA's Mars Reconnaissance Orbiter, 2004-present. Data analysis; Radiometric calibration; Science planning & targeting operations.
    - Post-Doctoral Research Scientist, Planetary Science Institute, Tucson, USA, 2009.
    - Post-Doctoral Research Scientist & Laboratory Instructor, Dept. Planetary Sciences & Space Research, University of Bern, Switzerland, 2004-2008. Helped supervise PhD student.
  - **Education**
    - Ph. D., Geological Sciences (Planetary Science), 2005 & M. Sc., 2001, Brown University, Providence RI, USA. Thesis: On the activity of water on Mars: Investigations into the groundwater system and the stability of ice in the crater-interior environment. Advisor: James W. Head III. Honors: First-Year Univ. Fellowship, Dissertation Fellowship, full member Sigma Xi, Sigma Xi Graduate Student Award: "Certificate of Merit for excellence in research and high potential for further contributions to science".
    - B. A., Geosciences, 1997, Williams College, Williamstown MA, USA. Honors: Summa cum laude, Phi Beta Kappa, inducted associate member Sigma Xi, Highest Honors (based on senior thesis). First year of university, 1993 – 1994: Yale University, New Haven CT, USA, full 9 courses, then transferred.
  - **Research - Mars Surface & Polar Geology, Behavior & History of Water & Ice, Seasonal Processes.**
    - ◆ Mars north polar (NP) geology (e.g., scarp erosion & landscape evolution; stratigraphy of layered deposits and basal materials; mass-wasting processes); ◆ Mars polar seasonal processes (e.g., spring CO<sub>2</sub> frost falls/avalanches at NP scarps; spring CO<sub>2</sub> out-gassing and fan activity at SP); ◆ Behavior/stability of water on Mars (e.g., development and implementation of numerical thermal modeling; crater-interior deposits around the NP and SP; candidate sublimation features at mid-latitudes); ◆ Development, testing, and implementation of technique to measure height/distance/and slope from pairs of points in HiRISE stereo pairs; ◆ Leader of HiRISE theme Climate Change: monitoring for active processes in/of H<sub>2</sub>O and CO<sub>2</sub> ices and potentially ice-rich terrains on time-scales of one to a few years.
  - **Selected Publications**
    - Holt, J. W., K. E. Fishbaugh, S. Byrne, S. Christian, K. Tanaka, P. Russell, K. E. Herkenhoff, A. Safaeinili, A., N. E. Putzig, R. Phillips, 2010, The construction of Chasma Boreale on Mars, *Nature*, 465, 7297, 446-449.
    - Fishbaugh, K. E., C. S. Hvidberg, S. Byrne, P. S. Russell, K. E. Herkenhoff, M. Winstrup, R. Kirk, 2010, First high-resolution stratigraphic column of the Martian north polar layered deposits, *Geophys. Res. Lett.*, 37, 7, L07201.
    - Thomas, N., C. J. Hansen, G. Portyankina, P. S. Russell, 2009, HiRISE Observations of Gas Sublimation-Driven Activity in Mars' Southern Polar Regions: II. Surficial Deposits and their Origins, *Icarus*, 205, 1, 296-310.
    - Russell, P., N. Thomas, S. Byrne, K. Herkenhoff, K. Fishbaugh, N. Bridges, C. Okubo, M. Milazzo, I. Daubar, C. Hansen, A. McEwen, 2008, Seasonally Active Frost-Dust Avalanches on a North Polar Scarp of Mars Captured by HiRISE, *Geophys. Res. Lett.*, 35, 23, L23204, doi:10.1029/2008GL035790.
    - Herkenhoff, K. E., S. Byrne, P. S. Russell, K. E. Fishbaugh, A. S. McEwen, 2007, Meter-Scale Morphology of the North Polar Region of Mars, *Science*, 317, 5845, 1711-1715, doi:10.1126/science.1143544.
    - McEwen, A., and 33 others, 2007, A Closer Look at Water-Related Geologic Activity on Mars, *Science*, 317, 5845, 1706-1709, doi: 10.1126/science.1143987.
    - Russell, P. S., and J. W. Head, 2007, The Martian Hydrologic System: Multiple Recharge Centers at Large Volcanic Provinces and the Contribution of Snowmelt to Outflow Channel Activity, *Planet. & Space Sci.*, 55, 3, 315-332.
    - Russell, P. S., and J. W. Head, 2003, Elysium-Utopia Flows as Mega-Lahars: A Model of Dike Intrusion, Cryosphere Cracking, and Water-Sediment Release, *J. Geophys. Res.*, 108, E6, 5064, doi:10.1029/2002JE001995.
    - Russell, P. S., and J. W. Head, 2002, The Martian Hydrosphere/Cryosphere System: Implications of the Absence of Hydrological Activity at Lyot Crater, *Geophys. Res. Lett.*, 29, 17, 1827, doi:10.1029/2002GL015178.

## 5. Current and Pending Support

### Current Support – Shane Byrne (PI)

Prof. Byrne is supported as a teaching faculty member at the University of Arizona for up to 9 months of the year (academic salary) by the state of Arizona. If more than three months of salary is available through research grants, Prof. Byrne will spend less than nine months teaching and more than three months doing research. Other projects that provide salary support during the proposed period are:

Project title	“Volatile migration and storage on Ceres and other large asteroids”
Name of PI on award	Dr. Shane Byrne
Program name	Planetary Geology and Geophysics
Sponsoring agency	NASA
Sponsor POC	Dr. Michael S. Kelley, (202)358-0607
Performance period	17 Dec 2007 - 16 Dec 2011
Total budget	\$91,000
<b>Support (person months)</b>	<b>1 (8.3%)</b>

Project title	“Short term climatic record from landscape evolution in the martian residual CO <sub>2</sub> cap”
Name of PI on award	Dr. Shane Byrne
Program name	Mars Data Analysis
Sponsoring agency	NASA
Sponsor POC	Dr. Robert Fogel, (202)358-2289
Performance period	7/1/2009 – 6/30/2012
Total budget	\$370,453
<b>Support (person-months)</b>	<b>2 (16.67%)</b>

Project title	“Quantitative Stratigraphy of north-polar basal layers”
Name of PI on award	Dr. Patrick Russell
Program name	Mars Data Analysis Program
Sponsoring agency	NASA
Sponsor POC	Dr. Robert Fogel, (202)358-2289
Performance period	7/1/2011 – 6/30/2015
Total budget	\$311,272
<b>Support (person-months)</b>	<b>1.2 (10%)</b>

Project title	High-Resolution Imaging Science Experiment
Name of PI on award	Dr. Alfred McEwen
Program name	Mars Reconnaissance Orbiter Mission
Sponsoring agency	NASA
Sponsor POC	Dr. Michael S. Kelley, (202)358-0607
Performance period	9/1/2010 – 8/31/2011
<b>Support (person-months)</b>	<b>1 (8.33%)</b>

Other projects that the PI is involved in provide no salary support and take minimal time commitment.



**Pending Support (proposals under review) – Shane Byrne (PI)**

Project title	“Constraining the Recent Climate of Mars through Analysis of Polar Craters” – <b>THIS PROPOSAL</b>
Name of PI on award	Dr. Shane Byrne
Program name	Mars Data Analysis Program
Sponsoring agency	NASA
Sponsor POC	Dr. Robert Fogel, (202)358-2289
Performance period	7/1/2011 – 6/30/2015
Total budget	\$455,357
Support (person-months)	2 (16.67%)

The PI is also a team-member of the recently selected HiSCI camera that will fly on the 2016 Mars Trace Gas Orbiter mission. The budget for this instrument has yet to be determined; however, it is currently anticipated that no salary money will be available to the PI until actual Mars operations commence (which will be after the end of this proposed work).

**Current Support – Patrick Russell (Co-I)**

Co-I Russell is currently partially supported by two grants awarded to supervisor Dr. John Grant:

1. **Title:** HiRise Mission: High Resolution Imaging Science Experiment – Phase E  
**Sponsor/Program:** NASA Mars Reconnaissance Orbiter Mission
2. **Title:** Potential of the Lunar Poles: Constraining Lunar Regolith Characteristics via GPR Investigation of Terrestrial Analogs  
**Sponsor/Program:** NASA Lunar Science Institute

Additional support to Co-I Russell is as follows:

1. **Title:** Quantitative Stratigraphy of North Polar Basal Layering  
**Sponsor/Program:** NASA Mars Data Analysis Program  
**Contact:** Robert Fogel 202-358-2289 rfogel@nasa.gov  
**Principal Investigator:** Patrick Russell (Smithsonian Institution)  
**Period of Performance:** 10/01/10 – 09/30/14  
**Budget:** \$ 321 K  
**P. R.'s Level of Effort:** 33% FTE
2. **Title:** Linking Visible and Radar Stratigraphy in the Martian Polar Deposits  
**Sponsor/Program:** NASA Mars Data Analysis Program  
**Contact:** Robert Fogel 202-358-2289 rfogel@nasa.gov  
**Principal Investigator:** Patrick Russell (Smithsonian Institution)  
**Period of Performance:** 09/08/10 – 09/02/12  
**Budget:** \$ 275 K  
**P. R.'s Level of Effort:** 33% FTE

A small award to Co-I Russell contains no salary support:

***Title:** Ground-Penetrating Radar Investigations at Meteor Crater*  
***Sponsor/Program:** Smithsonian Institution Endowment: Becker Fund*  
***Principal Investigator:** Patrick S. Russell*  
***Period of Performance:** 11/01/09 – 10/30/10*  
***Budget:** \$ 4 K*  
***P. R.'s Level of Effort:** Field work/travel/supplies – no salary.*

**Pending Support – Patrick Russell (Co-I)**

1. **Title:** Constraining the Recent Climate of Mars through Analysis of Polar Craters  
(THIS PROPOSAL)  
**Sponsor/Program:** NASA Mars Data Analysis Program  
**Contact:** Robert Fogel 202-358-2289 rfogel@nasa.gov  
**Principal Investigator:** Shane Byrne  
**Period of Performance:** 07/01/11 – 06/30/15  
**P. R.'s Level of Effort:** 10% FTE

**6. Budget Explanation**

**6.1 Budget Justification**

Personnel

We request funds to support for the following individuals: Shane Byrne (2 months) and 100% of a graduate student. Benefits for the graduate student are separated below into two figures as they are only partly subject to institutional overhead.

A subcontract to the Smithsonian (budget details below) will support co-investigator Dr. Patrick Russell at the 10% level. Only the first \$25K is subject to overhead at the university of Arizona.

<b>BUDGET SUMMARY</b> (Gov't - using proposed new rates non-SE - see proposed rates for 2011 and 2012)				2011	2012	2013	2013
Principle Investigator:	Patrick Russell	OSP Financial Analyst:					
Unit/Department:	NASM/CEPS	Designated Code:					
Sponsor:	NASA Mars Data Analysis Pro	Department ID:					
Award Start - End Date:	Jul 1, 2011 - Jun 30, 2015	Program Code:					
OSP Grant Administrator:	Violet Jones-Bruce	Proposal No.:					
<b>PERSONNEL COMPENSATION</b>							
1110 Salaries - Full time			6,863	7,069	7,281	7,499	
1111 Salaries - Part time			0	0	0	0	
1112 Salaries - Intermittent or Less than 90 days			0	0	0	0	
<b>TOTAL PERSONNEL COMPENSATION</b>			<b>6,863</b>	<b>7,069</b>	<b>7,281</b>	<b>7,499</b>	
<b>PERSONNEL BENEFITS *</b>							
(NCR Employees - duty station in the National Capital Region)							
1230 Pool Benefits	29.0% or 8.4%		1,990	2,029	2,090	2,152	
<b>TOTAL PERSONNEL BENEFITS</b>			<b>1,990</b>	<b>2,029</b>	<b>2,090</b>	<b>2,152</b>	
<b>TOTAL PERSONNEL COSTS (TPC)</b>			<b>8,853</b>	<b>9,098</b>	<b>9,371</b>	<b>9,651</b>	
<b>TOTAL DIRECT COSTS (TDC)</b>			<b>8,853</b>	<b>9,098</b>	<b>9,371</b>	<b>9,651</b>	
<b>INDIRECT COSTS *</b>							
3520 G&C	21.1% X TPC		1,868	2,020	2,080	2,143	
3510 G&A	10.8% X (TDC + G&C)		1,158	1,134	1,168	1,203	
<b>TOTAL INDIRECT COSTS</b>			<b>3,026</b>	<b>3,154</b>	<b>3,248</b>	<b>3,346</b>	
<b>TOTAL COSTS</b>			<b>11,879</b>	<b>12,252</b>	<b>12,619</b>	<b>12,997</b>	

Travel Expenses

Support for travel to one domestic conference per year, such as the AGU or LPSC conferences (San Francisco, CA or Houston, TX) for the PI and graduate student has been included. The estimated costs below are based on prior travel to an AGU meeting in San Francisco, CA.

Daily expenses		
Meals & Incidentals	\$59.00	
Accommodation	\$140.00	\$199.00
Number of Days		5
<b>Total daily expenses</b>		<b>\$995.00</b>
Non-daily expenses		
Airfare (Tucson – San Francisco)	\$230.00	
Conference-airport transport	\$20.00	
Conference abstract submission	\$50.00	
Conference registration	\$380.00	\$680.00
<b>Travel total</b>		<b>\$1,675.00</b>

Publication Charges

Funds for publication charges of papers that will describe our results are included. The amount of \$1500 is based on the PI’s recent experience with the *Journal of Geophysical Research (Planets)*.

Computer Maintenance


Funds (\$500/year) to replace computer components that fail (such as hard drives) are requested.

Equipment Purchase

A once-off computer purchase for the graduate student to perform their proposed tasks has been included in year 1. Purchases of equipment that exceed \$5K are not subject to institutional overhead. Computer priced is Mac Pro desktop with a dual quad-core 2.4 GHz processor, 16 GB RAM, four 2TB hard-drive (display is available at no cost to this grant). Total, including sales tax and University of Arizona discount, is \$6515 (quote provided by the Apple website, see below).

**Apple Store** Questions? Need Advice? Call 1-800-MY-APPLE

Items in Your Cart

	<b>Mac Pro</b>	\$5,999.00	1	\$5,999.00
--	----------------	------------	---	------------

Ships: 5-7 business days  
Part number: Z0LG

**Configuration**

- Two 2.4GHz Quad-Core Intel Xeon "Westmere" (8 cores)
- 16GB (8x2GB)
- Mac Pro RAID Card
- 2TB 7200-rpm Serial ATA 3Gb/s hard drive
- 2TB 7200-rpm Serial ATA 3Gb/s hard drive
- 2TB 7200-rpm Serial ATA 3Gb/s hard drive
- 2TB 7200-rpm Serial ATA 3Gb/s hard drive
- ATI Radeon HD 5770 1GB
- One 18x SuperDrive
- Apple Magic Mouse
- Apple Keyboard with Numeric Keypad (English) & User's Guide
- COUNTRY KIT

Shipping Zip 8574

Ship Method  
Standard Shipping —Free

Cart subtotal	\$5,999.00
Free Shipping	\$0.00
Estimated Tax	\$515.91
<b>Order Total</b>	<b>\$6,514.91</b>

6.2 Budget Amounts

MDAP 2010 Budget 4.0 Years 7/1/2011 to 6/30/2015	Rates and Percentage Contribution	Year 1		Year 2		Year 3		Year 4	
		Amounts	Subtotals	Amounts	Subtotals	Amounts	Subtotals	Amounts	Subtotals
<b>Personnel</b>									
<b>Salaries</b>									
PI - Professor Byrne (2 months)	16.7%	15,889		15,889		15,889		15,889	
Graduate Student	100.0%	28,738		28,738		28,738		28,738	
<b>Benefits (not subject to overhead)</b>									
Graduate Student	30.7%	8,823		8,823		8,823		8,823	
<b>Benefits (Subject to overhead)</b>									
Graduate Student	11.9%	3,420		3,420		3,420		3,420	
PI - Professor Byrne	28.4%	4,512	61,382	4,512	61,382	4,512	61,382	4,512	61,382
<b>Publication charges</b>									
Estimate one JGR/Icarus paper		1,500	1,500	1,500	1,500	1,500	1,500	1,500	1,500
<b>Maintenance and Material Expenses</b>									
Computer maintenance and upgrades		500	500	500	500	500	500	500	500
<b>Travel and Meetings</b>									
One domestic conference - PI Byrne		1,675		1,675		1,675		1,675	
One domestic conference - Graduate Student		1,675	3,350	1,675	3,350	1,675	3,350	1,675	3,350
<b>Equipment Purchase</b>									
Computer workstation (not subject to overhead)		6,515		6,515					
<b>Subcontracts</b>									
Smithsonian Institute - Co-I Russel (1.2 months) (First \$25K subject to overhead)		11,879	11,879	12,252	12,252	12,619	12,619	12,997	12,997
<b>TOTAL DIRECT COSTS</b>			<b>85,126</b>		<b>78,984</b>		<b>79,351</b>		<b>79,729</b>
<b>Indirect Costs</b>									
Direct costs not subject to overhead		15,338	0	8,823	0	20,573	0	21,820	0
Direct costs subject to overhead rate of	51.5%	69,788	35,941	70,161	36,133	58,778	30,271	57,909	29,823
<b>TOTAL ANNUAL COST</b>			<b>121,067</b>		<b>115,117</b>		<b>109,621</b>		<b>109,552</b>
<b>TOTAL FOUR YEAR COST</b>					<b>455,357</b>				